

## ELECTRONIC SUPPLEMENTARY INFORMATION

### **Towards improved halogenated BODIPY photosensitizers: clues on structural design and heavy atom substitution pattern**

Antonio J. Sánchez, Eduardo Palao, Antonia R. Agarrabeitia, María J. Ortiz\* and  
David García-Fresnadillo\*

Departamento de Química Orgánica I, Facultad de Ciencias Químicas, Universidad Complutense de  
Madrid, E-28040 Madrid, Spain.

E-mail: [dgfresna@ucm.es](mailto:dgfresna@ucm.es)

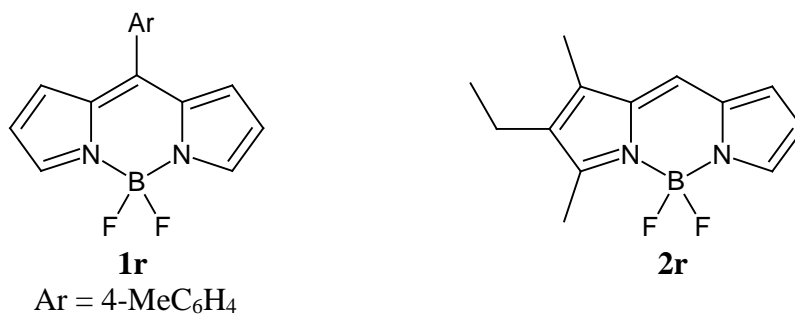
### CONTENTS

1. Experimental section. General information.....	S2
2. Synthesis and characterization of BODIPY dyes.....	S3
3. <sup>1</sup> H NMR and <sup>13</sup> C NMR spectra.....	S5
4. UV-VIS absorption spectra in acetonitrile.....	S9
5. Calculation of the singlet oxygen production quantum yields.....	S12
6. Calculation of the photodegradation rate constants and quantum yields.....	S14
7. Chemical actinometry.....	S17
8. Principal component analyses.....	S19

## 1. Experimental section. General information.

*Synthesis:* All starting materials and reagents were commercially obtained, unless otherwise indicated, and used without further purifications. Common solvents were dried and distilled by standard procedures. Flash chromatography was performed using silica gel (230-400 mesh). NMR spectra were recorded at 20 °C, and the residual solvent peaks used as internal standards. FTIR spectra were obtained from neat samples using the ATR technique. Mass spectra (MS) and high resolution mass spectrometry (HRMS) were performed using the EI technique.

BODIPYs **1r**,<sup>1</sup> **2r**,<sup>2</sup> **3-5**,<sup>3</sup> **7**,<sup>3</sup> and **11-14**<sup>4</sup> were synthesized by the described methods. BODIPYs **6**<sup>5</sup> and **8**<sup>6</sup> were synthesized by a modification of the methods previously described for such compounds.



<sup>1</sup> A. Cui, X. Peng, J. Fan, X. Chen, Y. Wu and B. Guo, *J. Photochem. Photobiol. A*, 2007, **186**, 85-92.

<sup>2</sup> (a) E. Vos de Wael, J. A. Pardoën, J. A. van Koeveringe and J. Lugtenburg, *Recl. Trav. Chim. Pays-Bas-J. R. Neth. Chem. Soc.*, 1977, **96**, 306-309. (b) S. M. Crawford and A. Thompson, *Org. Lett.*, 2010, **12**, 1424-1427.

<sup>3</sup> M. Rajeswara Rao, K. V. Pavan Kumar and M. Ravikanth, *J. Organomet. Chem.*, 2010, **695**, 863-869.

<sup>4</sup> M. J. Ortiz, A. R. Agarrabeitia, G. Duran-Sampedro, J. Bañuelos Prieto, T. Arbeloa Lopez, W. A. Massad, H. A. Montejano, N. A. Garcia and I. Lopez Arbeloa, *Tetrahedron*, 2012, **68**, 1153-1162.

<sup>5</sup> E. Heyer, P. Retailleau and R. Ziessel, *Org. Lett.*, 2014, **16**, 2330-2333.

<sup>6</sup> V. Lakshmi and M. Ravikanth, *Eur. J. Org. Chem.*, 2014, 5757-5766.

## 2. Synthesis and characterization of BODIPY dyes.

**General procedure for the synthesis of bromo-BODIPYs.** To a solution of BODIPY (1 equiv.) in dry CH<sub>2</sub>Cl<sub>2</sub> liquid bromine (0.9-100 equiv.) in dry CH<sub>2</sub>Cl<sub>2</sub> was slowly added, and the mixture was stirred until the complete consumption of the starting material was observed by TLC. The reaction crude was washed with an aqueous saturated solution of sodium thiosulfate and extracted by CH<sub>2</sub>Cl<sub>2</sub>. Organic layers were dried over MgSO<sub>4</sub>, filtered and concentrated to dryness under vacuum. The brominated BODIPYs were purified by flash chromatography on silica gel using hexane/EtOAc as eluent.

**1,2-Dibromo-6-ethyl-4,4-difluoro-5,7-dimethyl-4-bora-3a,4a-diaza-s-indacene (1) and 2,3-dibromo-6-ethyl-4,4-difluoro-5,7-dimethyl-4-bora-3a,4a-diaza-s-indacene (2).** According to the general procedure, BODIPY **2r**<sup>2</sup> (50 mg, 0.20 mmol) in dry CH<sub>2</sub>Cl<sub>2</sub> (10 mL) and liquid bromine (0.09 mL, 0.18 mmol, 2 M solution in CH<sub>2</sub>Cl<sub>2</sub>) were reacted for 3 h. Flash chromatography using hexane/CHCl<sub>3</sub> (9:1) afforded BODIPY **1** (15 mg, 28%) as a red solid, and BODIPY **2** (29 mg, 55%) as a red solid. Our characterization data for BODIPY **2** are in excellent agreement with those reported very recently by Hao and co-workers.<sup>7</sup>

*Compound 1:* <sup>1</sup>H NMR (700 MHz, CDCl<sub>3</sub>) δ/ppm: 7.37 (s, 1H, CH), 7.04 (s, 1H, CH), 2.50 (s, 3H, CH<sub>3</sub>), 2.36 (q, *J* = 7.7 Hz, 2H, CH<sub>2</sub>), 2.17 (s, 3H, CH<sub>3</sub>), 1.03 (t, *J* = 7.7 Hz, 3H, CH<sub>3</sub>); <sup>13</sup>C NMR (176 MHz, CDCl<sub>3</sub>) δ/ppm: 167.5 (C), 142.7 (C), 137.7 (C), 136.6 (C), 136.3 (C), 134.8 (CH), 130.1 (C), 120.4 (CH), 105.1 (C), 17.3 (CH<sub>2</sub>), 14.0 (CH<sub>3</sub>), 13.7 (CH<sub>3</sub>), 9.7 (CH<sub>3</sub>); FTIR (neat): 2951, 1530, 1481, 1345, 1233, 1104, 991 cm<sup>-1</sup>; HRMS-EI: for C<sub>13</sub>H<sub>13</sub>BBr<sub>2</sub>F<sub>2</sub>N<sub>2</sub> 403.9505 calcd., 403.9510 found.

*Compound 2:* <sup>1</sup>H NMR (700 MHz, CDCl<sub>3</sub>) δ/ppm: 6.94 (s, 1H, CH), 6.82 (s, 1H, CH), 2.62 (s, 3H, CH<sub>3</sub>), 2.44 (q, *J* = 7.7 Hz, 2H, CH<sub>2</sub>), 2.21 (s, 3H, CH<sub>3</sub>), 1.12 (t, *J* = 7.7 Hz, 3H, CH<sub>3</sub>); <sup>13</sup>C NMR (176 MHz, CDCl<sub>3</sub>) δ/ppm: 166.7 (C), 141.9 (C), 137.0 (C), 136.4 (C), 132.4 (C), 124.7 (CH), 123.4 (C), 121.0 (CH), 106.5 (C), 17.3 (CH<sub>2</sub>), 14.0 (CH<sub>3</sub>), 13.6 (CH<sub>3</sub>), 9.5 (CH<sub>3</sub>); FTIR (neat): 2941, 1531, 1483, 1328, 1229, 1112, 993 cm<sup>-1</sup>; HRMS-EI: for C<sub>13</sub>H<sub>13</sub>BBr<sub>2</sub>F<sub>2</sub>N<sub>2</sub> 403.9505 calcd., 403.9509 found.

**2,6-Dibromo-4,4-difluoro-8-(4-tolyl)-4-bora-3a,4a-diaza-s-indacene (6).** According to the general procedure, BODIPY **1r**<sup>1</sup> (100 mg, 0.35 mmol) in dry CH<sub>2</sub>Cl<sub>2</sub> (15 mL) and liquid bromine (0.39 mL, 0.78 mmol, 2 M solution in CH<sub>2</sub>Cl<sub>2</sub>) were reacted for 1 h. Flash chromatography using hexane/EtOAc (98:2) afforded, by order of elution, BODIPY **6**<sup>5</sup> (98 mg, 63%) as a red solid and the starting product **1r** (12 mg, 12%). The spectroscopic data agree with those previously described.

**2,3,5,6-Tetrabromo-4,4-difluoro-8-(4-tolyl)-4-bora-3a,4a-diaza-s-indacene (8).** According to the general procedure, BODIPY **1r**<sup>1</sup> (100 mg, 0.35 mmol) in dry CH<sub>2</sub>Cl<sub>2</sub> (15 mL) and liquid bromine (0.9 mL, 1.77 mmol, 2 M solution in CH<sub>2</sub>Cl<sub>2</sub>) were reacted for 1.5 h. Flash chromatography using hexane/EtOAc (98:2) afforded BODIPY **8**<sup>6</sup> (168 mg, 80%) as a purple solid. The spectroscopic data agree with those previously described.

**1,2,3,5,6,7-Hexabromo-4,4-difluoro-8-(4-tolyl)-4-bora-3a,4a-diaza-s-indacene (9).** According to the general procedure, BODIPY **1r**<sup>1</sup> (100 mg, 0.35 mmol) in dry CH<sub>2</sub>Cl<sub>2</sub> (15 mL) and liquid bromine (18 mL, 35 mmol, 2 M solution in CH<sub>2</sub>Cl<sub>2</sub>) were reacted for 5 h. Flash chromatography using hexane/EtOAc (98:2) afforded BODIPY **9** (122 mg, 45%) as a purple solid. <sup>1</sup>H NMR (700 MHz, CDCl<sub>3</sub>) δ/ppm: 7.27 (d, *J* = 7.7 Hz, 2H, 2CH), 7.04 (d, *J* = 7.7 Hz, 2H, 2CH), 2.41 (s, 3H, CH<sub>3</sub>); <sup>13</sup>C NMR (176 MHz, CDCl<sub>3</sub>) δ/ppm: 143.4 (C), 140.8 (C), 135.0 (C), 131.5 (C), 130.3 (CH), 128.3 (CH),

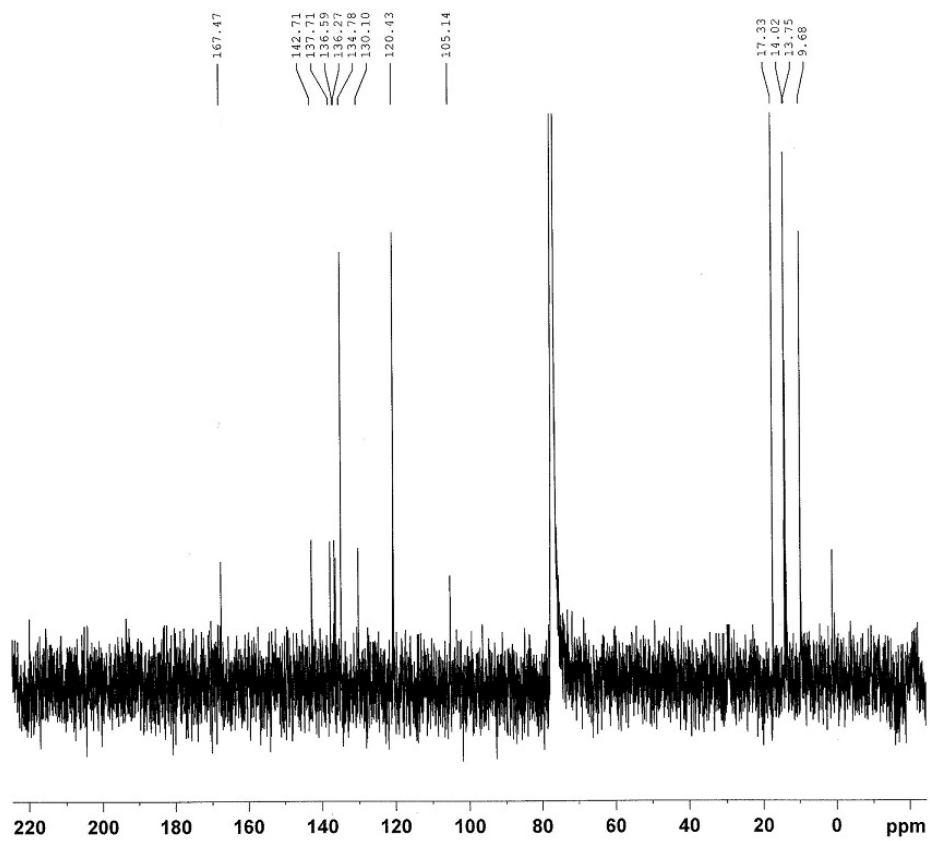
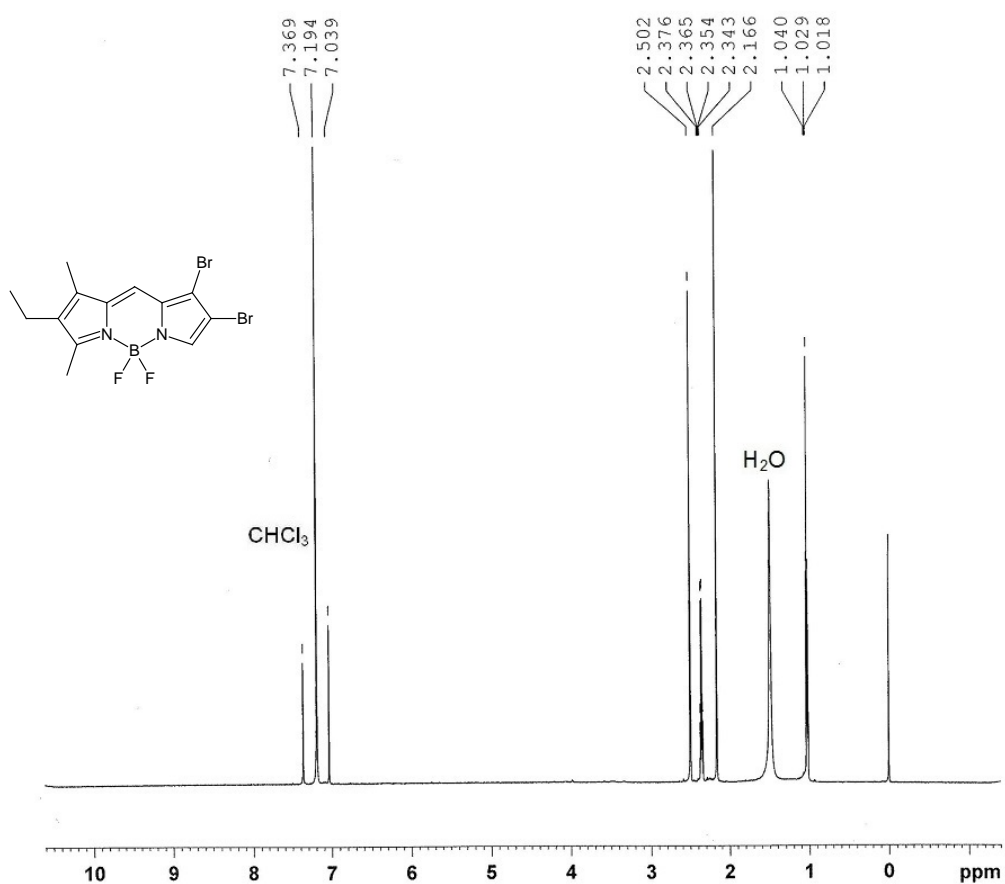
<sup>7</sup> Z. Feng, L. Jiao, Y. Feng, C. Yu, N. Chen, Y. Wei, X. Mu and E. Hao, *J. Org. Chem.*, 2016, **81**, 6281-6291.

126.4 (CH), 124.0 (C), 117.6 (C), 21.7 (CH<sub>3</sub>); FTIR (neat): 2921, 1532, 1515, 1361, 1260, 1131, 1019 cm<sup>-1</sup>; MS (EI): *m/z* 755.6 (M<sup>+</sup>, 100), 753.6 (72), 757.6 (69), 674.7 (48), 595.7 (42), 435.9 (25), 201.1 (26); HRMS-EI: for C<sub>16</sub>H<sub>7</sub>BBr<sub>6</sub>F<sub>2</sub>N<sub>2</sub> 749.5768 calcd., 749.5773 found.

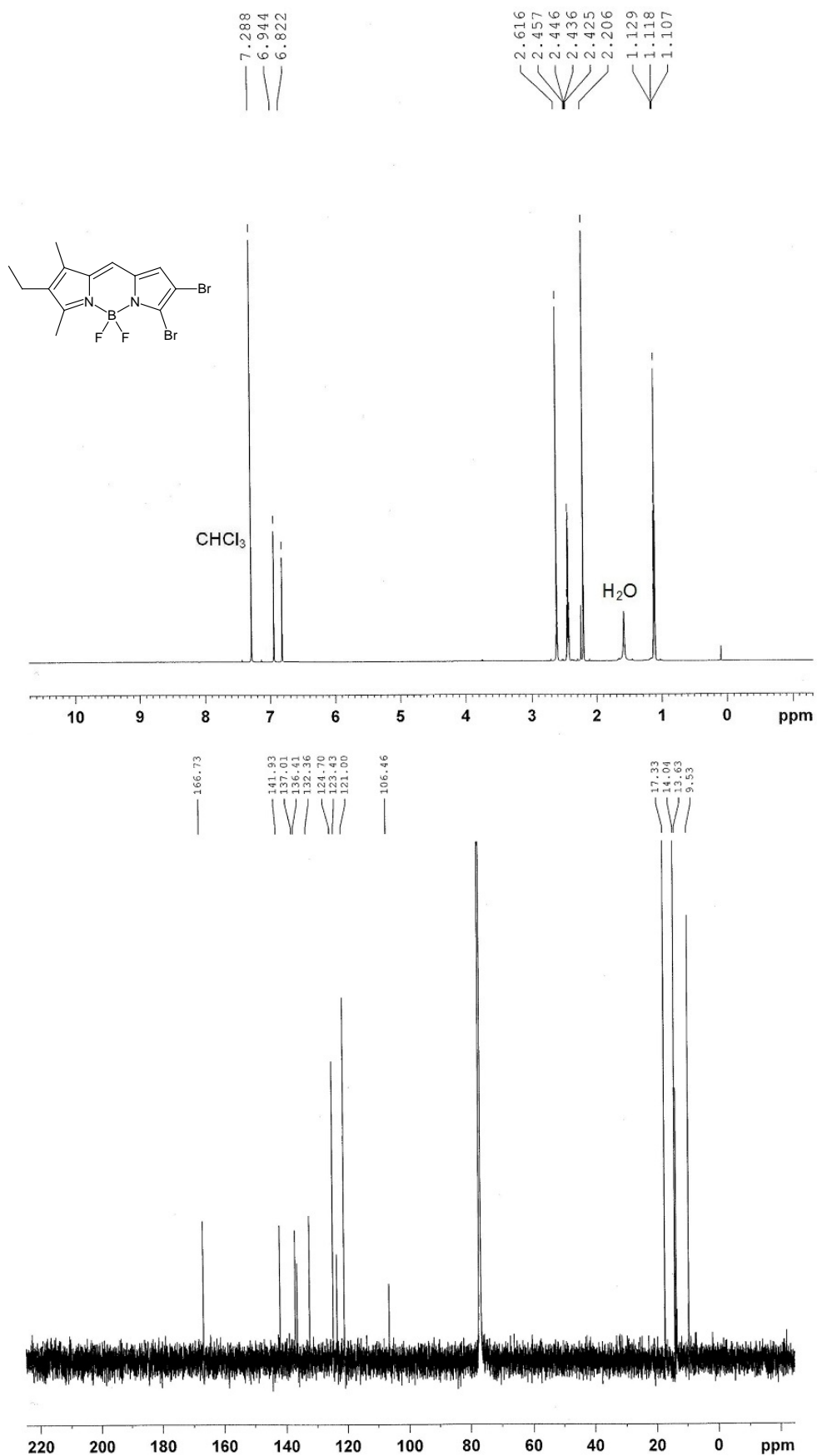
**1,2,6,7-Tetrabromo-3,5-bis(dimethoxycarbonylmethyl)-4,4-difluoro-8-(4-tolyl)-4-bora-3a,4a-diaza-s-indacene (10).** A solution of BODIPY **9** (20 mg, 0.03 mmol), dimethyl malonate (0.03 mL, 0.24 mmol) and NaH (2 mg, 0.09 mmol) in CH<sub>3</sub>CN (20 mL) were refluxed for 5 h. The solvent was removed under reduced pressure and the resulting mixture was dissolved in EtOAc and washed with H<sub>2</sub>O. The extract was dried over MgSO<sub>4</sub>, filtered and concentrated to dryness. Flash chromatography on silica gel using hexane/EtOAc (8:2) afforded BODIPY **10** (10 mg, 40%) as a purple solid. <sup>1</sup>H NMR (700 MHz, CDCl<sub>3</sub>) δ/ppm: 7.29 (d, *J* = 7.7 Hz, 2H, 2CH), 7.08 (d, *J* = 7.7 Hz, 2H, 2CH), 5.48 (s, 2H, 2CH), 3.76 (s, 12H, 4CH<sub>3</sub>), 2.41 (s, 3H, CH<sub>3</sub>); <sup>13</sup>C NMR (176 MHz, CDCl<sub>3</sub>) δ/ppm: 165.0 (COO), 148.5 (C), 147.0 (C), 140.7 (C), 130.3 (CH), 130.0 (C), 128.1 (CH), 127.0 (C), 125.5 (C), 115.2 (C), 53.6 (CH<sub>3</sub>O), 51.3 (CH), 21.7 (CH<sub>3</sub>); FTIR (neat): 2955, 1746, 1519, 1434, 1258, 1134, 1104, 1024, 1004, 931 cm<sup>-1</sup>; HRMS-EI: for C<sub>26</sub>H<sub>21</sub>BBr<sub>4</sub>F<sub>2</sub>N<sub>2</sub>O<sub>8</sub> 853.8090 calcd., 853.8096 found.

### 3. $^1\text{H}$ NMR and $^{13}\text{C}$ NMR spectra.

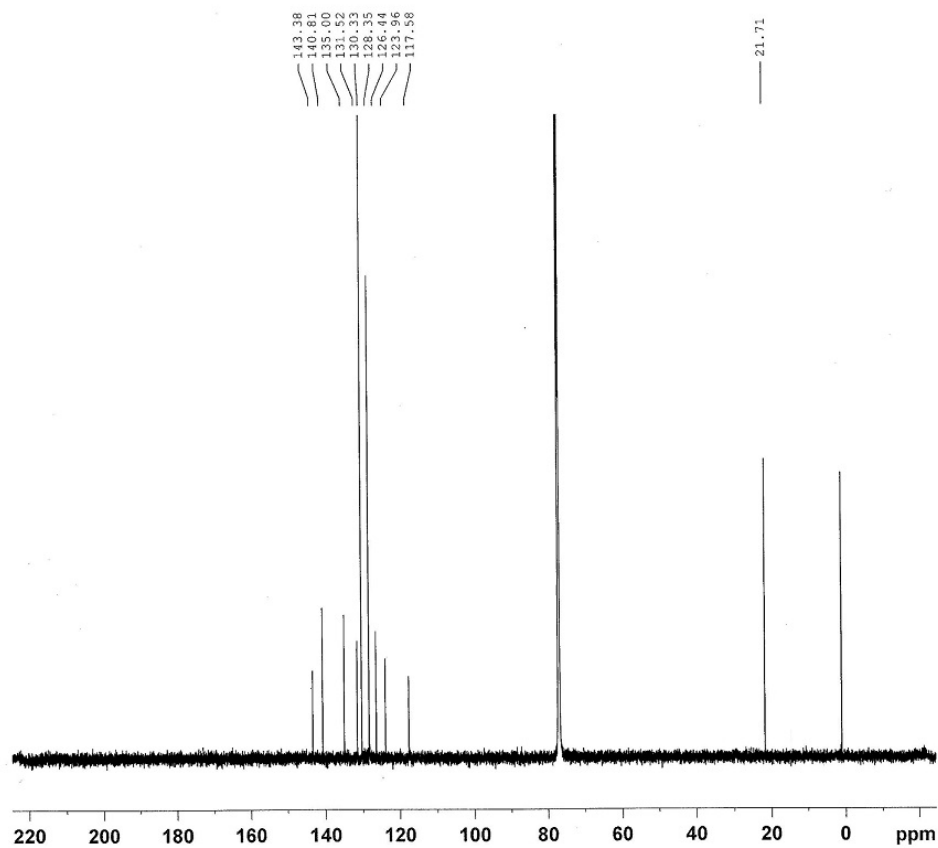
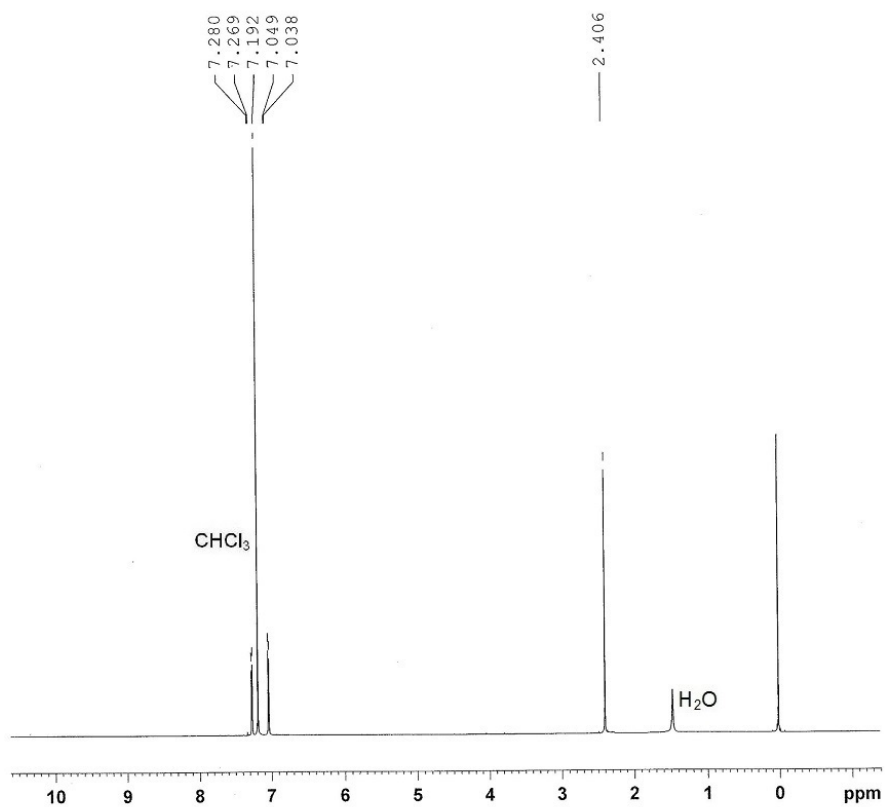
$^1\text{H}$  (700 MHz,  $\text{CDCl}_3$ ) and  $^{13}\text{C}$  (176 MHz,  $\text{CDCl}_3$ ) spectra of **1**



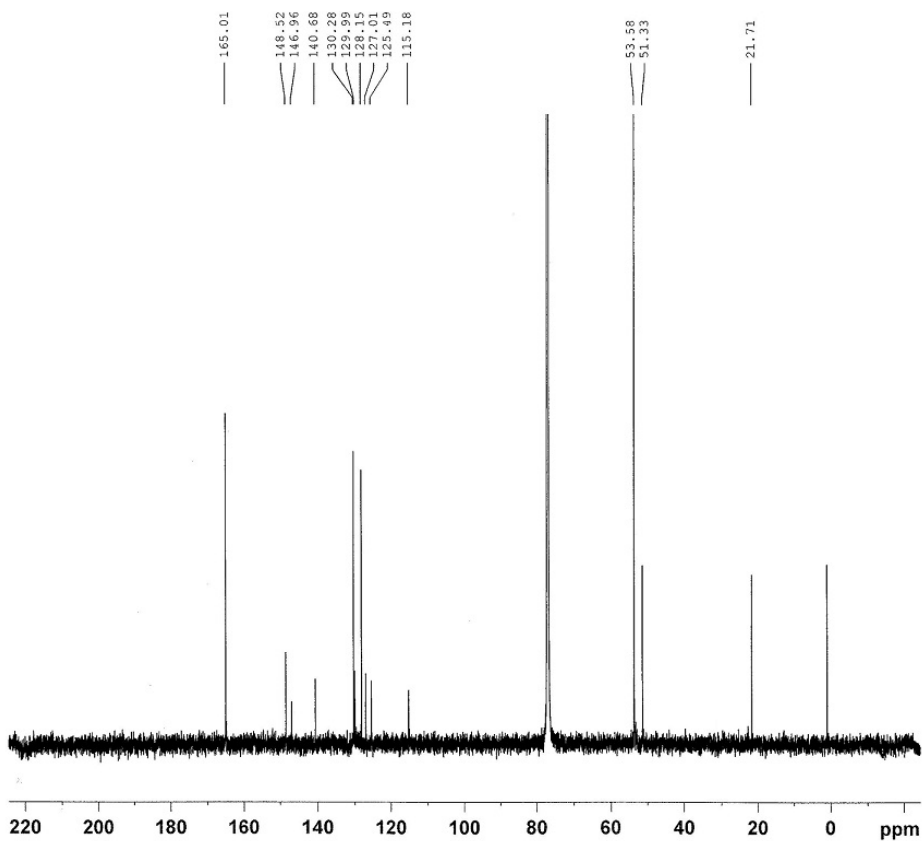
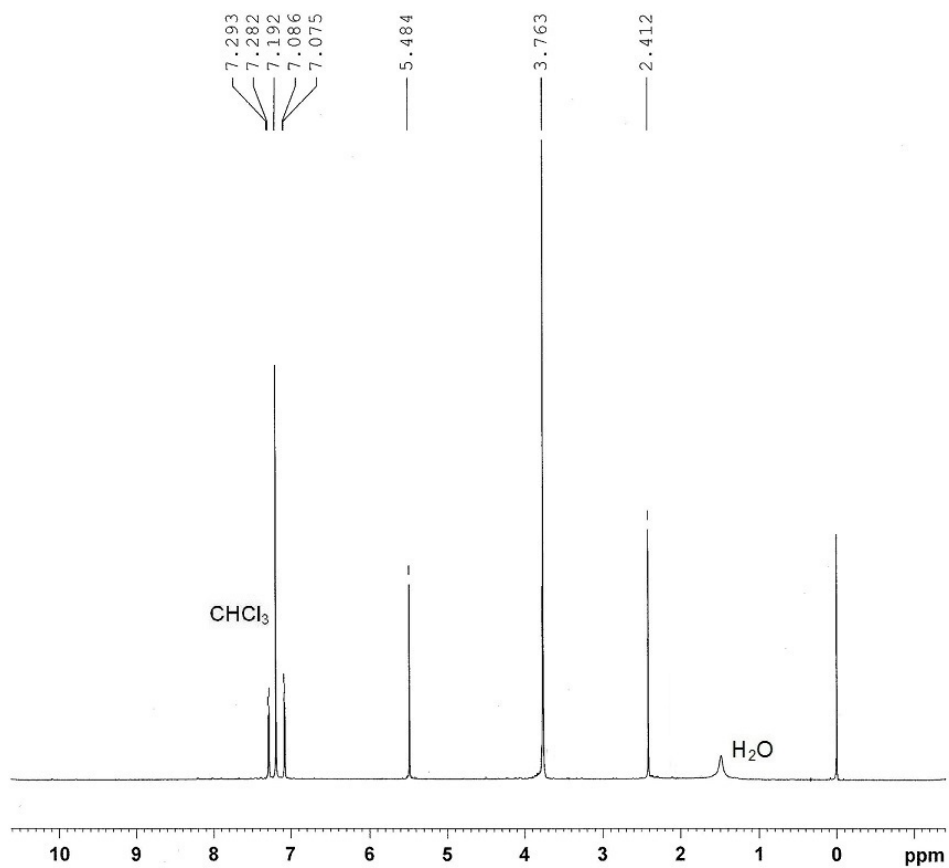
$^1\text{H}$  (300 MHz,  $\text{CDCl}_3$ ) and  $^{13}\text{C}$  (75 MHz,  $\text{CDCl}_3$ ) spectra of **2**



$^1\text{H}$  (700 MHz,  $\text{CDCl}_3$ ) and  $^{13}\text{C}$  (176 MHz,  $\text{CDCl}_3$ ) spectra of **9**



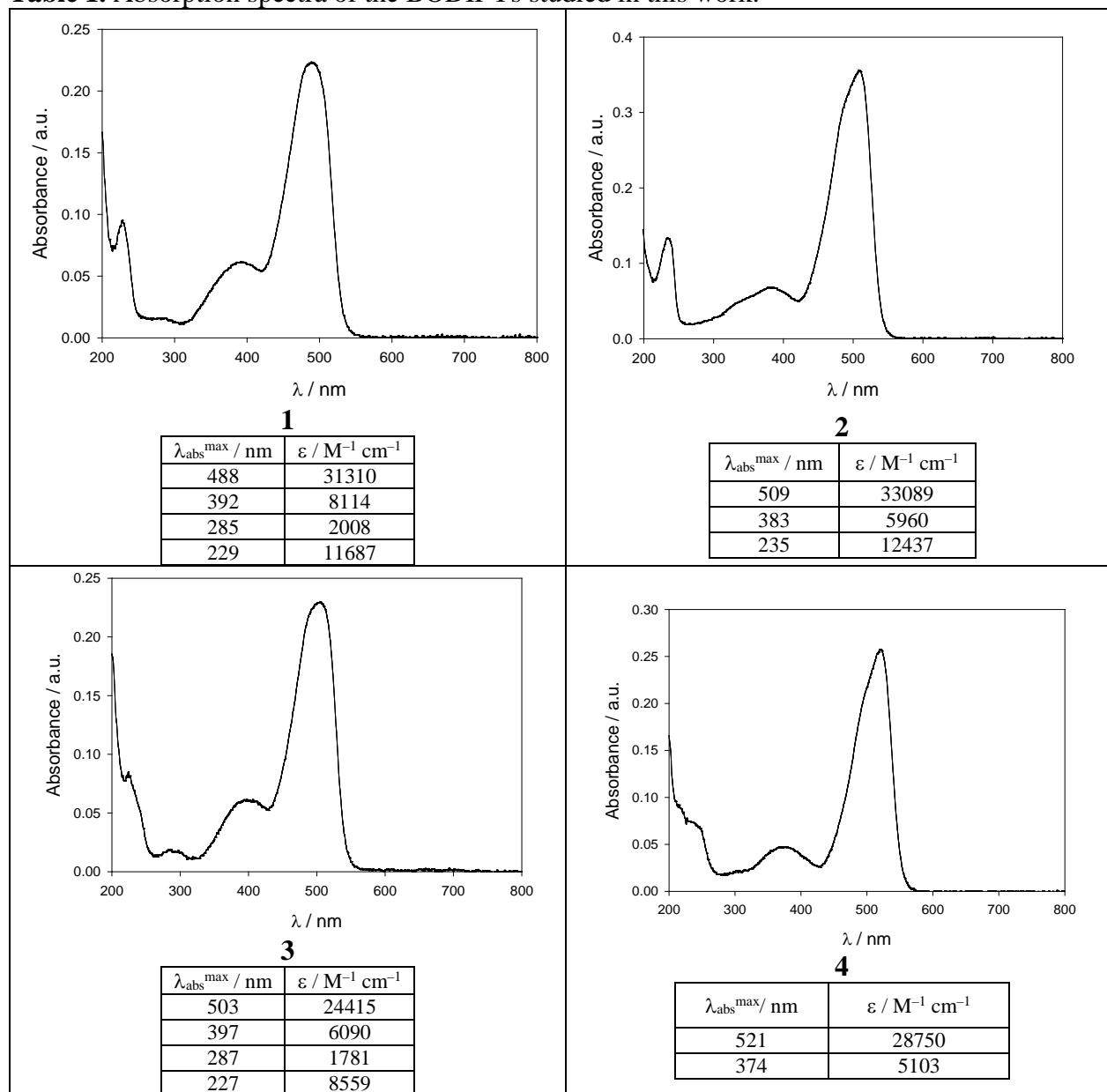
$^1\text{H}$  (700 MHz,  $\text{CDCl}_3$ ) and  $^{13}\text{C}$  (176 MHz,  $\text{CDCl}_3$ ) spectra of **10**

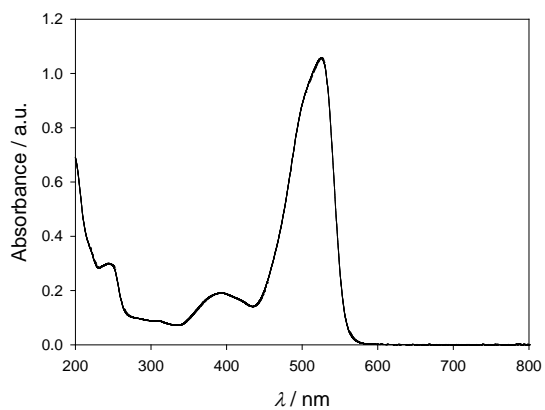


#### 4. UV-VIS absorption spectra in acetonitrile.

The quartz cuvettes used in absorption experiments were 10.00 mm lighth path or 1.00 mm lighth path. Absorption maxima uncertainty  $\pm 2$  nm, from duplicate samples,  $\epsilon$  uncertainty  $\pm 10\%$ .

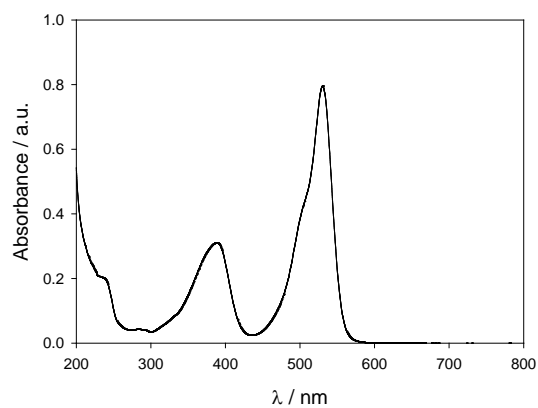
**Table 1.** Absorption spectra of the BODIPYs studied in this work.





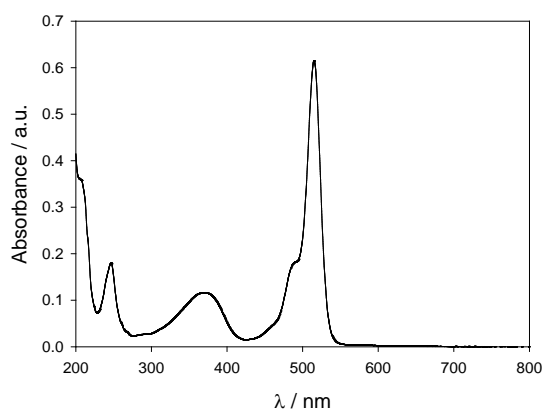
**5**

$\lambda_{\text{abs}}^{\text{max}} / \text{nm}$	$\epsilon / \text{M}^{-1} \text{cm}^{-1}$
525	33938
393	6122
243	9625



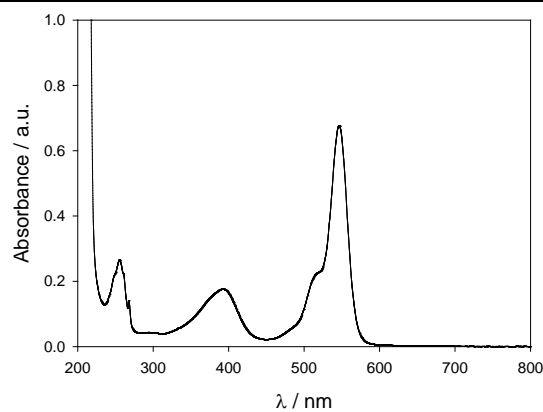
**6**

$\lambda_{\text{abs}}^{\text{max}} / \text{nm}$	$\epsilon / \text{M}^{-1} \text{cm}^{-1}$
531	46210
389	18042



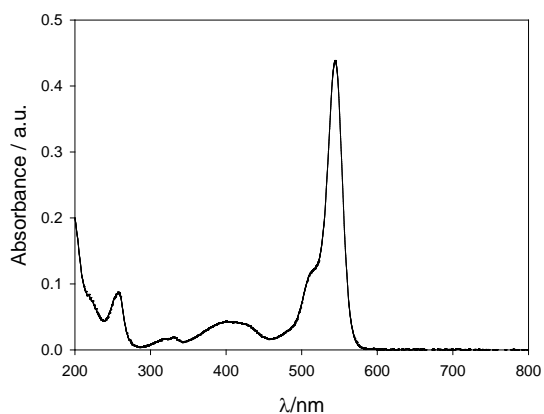
**7**

$\lambda_{\text{abs}}^{\text{max}} / \text{nm}$	$\epsilon / \text{M}^{-1} \text{cm}^{-1}$
515	75747
371	13456
247	21684



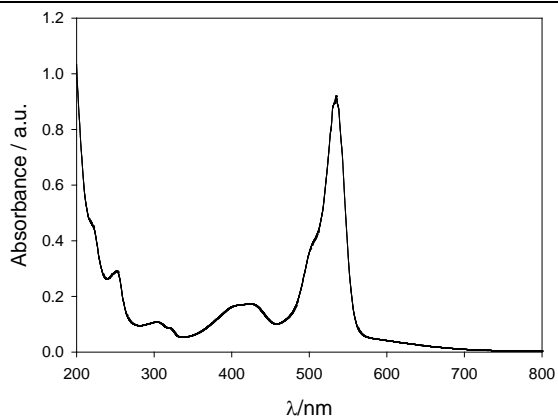
**8**

$\lambda_{\text{abs}}^{\text{max}} / \text{nm}$	$\epsilon / \text{M}^{-1} \text{cm}^{-1}$
546	57287
393	13541
255	22440



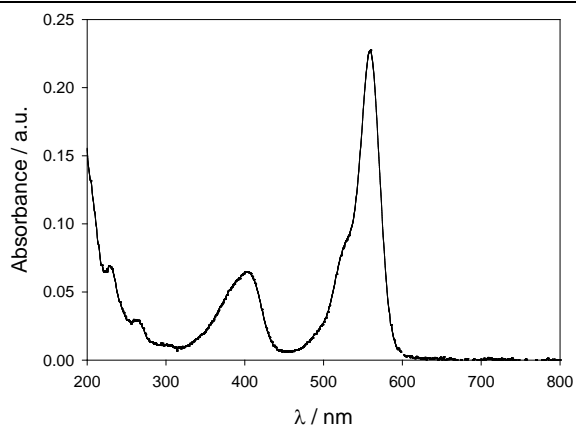
**9**

$\lambda_{\text{abs}}^{\text{max}} / \text{nm}$	$\epsilon / \text{M}^{-1} \text{cm}^{-1}$
544	70519
403	7431
317	3200
257	15632



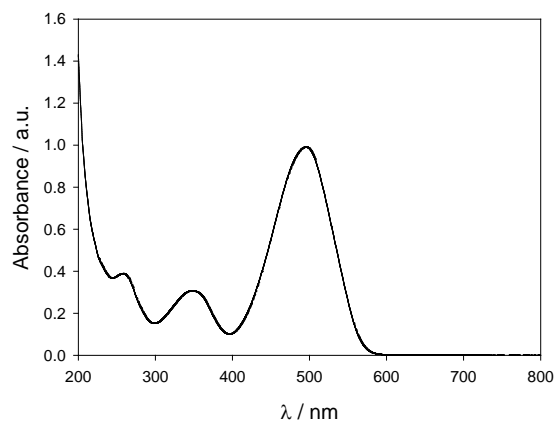
**10**

$\lambda_{\text{abs}}^{\text{max}} / \text{nm}$	$\epsilon / \text{M}^{-1} \text{cm}^{-1}$
534	23214
423	4493
303	3527
251	7659



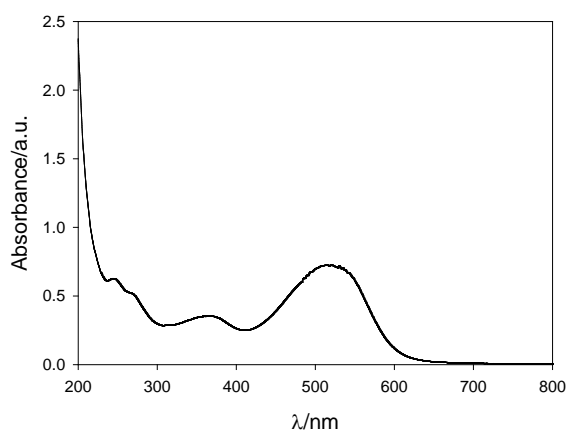
**11**

$\lambda_{\text{abs}}^{\text{max}} / \text{nm}$	$\epsilon / \text{M}^{-1} \text{cm}^{-1}$
559	39241
404	12188
263	6521
228	14218



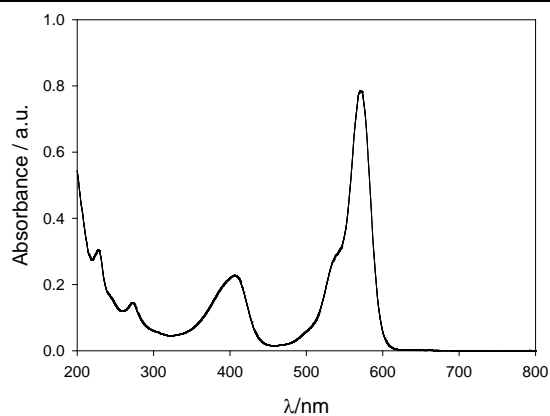
**12**

$\lambda_{\text{abs}}^{\text{max}} / \text{nm}$	$\epsilon / \text{M}^{-1} \text{cm}^{-1}$
497	30771
348	9537
258	12094



**13**

$\lambda_{\text{abs}}^{\text{max}} / \text{nm}$	$\epsilon / \text{M}^{-1} \text{cm}^{-1}$
518	14808
363	6876
244	11924



**14**

$\lambda_{\text{abs}}^{\text{max}} / \text{nm}$	$\epsilon / \text{M}^{-1} \text{cm}^{-1}$
573	43793
404	12113
282	12126
227	16632

## 5. Calculation of the singlet oxygen production quantum yields.

The singlet oxygen photosensitizers were dissolved in acetonitrile (99.85%, gradient 240 nm far UV, HPLC grade). The quartz cuvettes used were 10.00 mm lighth path.

Singlet oxygen emission intensities and lifetimes in acetonitrile were determined using a laser flash photolysis system equipped with a Nd-YAG laser and a NIR PMT detector.<sup>8</sup> The emission decay traces (10 shots/sample,  $\lambda_{exc}$  532 nm,  $\lambda_{em}$  1270 nm) were analyzed using the Marquardt algorithm included in the instrument software package for decay analysis.

Singlet oxygen production quantum yields of BODIPY derivatives in acetonitrile were determined relative to rose Bengal (RB) as a reference photosensitizer ( $\Phi_{\Delta} = 0.71$ )<sup>3</sup> by recording the singlet oxygen luminescence decay curves following pulse laser excitation of RB solution and the corresponding BODIPY photosensitizer solutions, respectively. The luminescence intensities at 1270 nm were measured under identical experimental conditions from identical laser pulses, from matched solutions (absorbance  $0.100 \pm 0.009$  at 532 nm) and extrapolated back to zero time. The relationship used is shown in eq. [1]:

$$\frac{\Phi_{\Delta}^{app}}{\Phi_{\Delta}^{Ref}} = \frac{L_{\Delta}}{L_{\Delta}^{Ref}} \quad [1]$$

where  $\Phi_{\Delta}^{app}$  is the apparent singlet oxygen production quantum yield for the BODIPY photosensitizer (uncorrected for the singlet oxygen quenching by the sensitizer itself),  $\Phi_{\Delta}^{Ref}$  is the singlet oxygen production quantum yield of RB in acetonitrile, and  $L_{\Delta}$  and  $L_{\Delta}^{Ref}$  are the singlet oxygen luminescence intensities extrapolated back to zero time for the BODIPY photosensitizer and the reference photosensitizer RB, respectively.<sup>9</sup> In order to eliminate any possible nonlinear effects, this ratio was extrapolated to zero laser intensity.<sup>10</sup> Therefore,  $L_{\Delta}$  (and also  $L_{\Delta}^{Ref}$ ) were measured as a function of the laser fluence ( $P_{Laser}$ ), and the ratio of the slopes ( $S$ ) of the linear plots ( $L_{\Delta} = S \times P_{Laser}$ ) shown in Fig. 1 were used in eq. [2] to give  $\Phi_{\Delta}^{app}$  values relative to RB reference sensitizer.

$$\frac{\Phi_{\Delta}^{app}}{\Phi_{\Delta}^{Ref}} = \frac{S_{\Delta}}{S_{\Delta}^{Ref}} \quad [2]$$

<sup>8</sup> (a) E. Díez-Mato, F. C. Cortezón-Tamarit, S. Bogialli, D. García-Fresnadillo and M. D. Marazuela, *Appl. Cat. B: Environ.* 2014, **160-161**, 445-455. (b) A. J. Sánchez-Arroyo, Z. D. Pardo, F. Moreno-Jiménez, A. Herrera, N. Martín and D. García-Fresnadillo, *J. Org. Chem.*, 2015, **80**, 10575-10584.

<sup>9</sup> F. Wilkinson, W. P. Helman and A. B. Ross, *J. Phys. Chem. Ref. Data*, 1993, **22**, 113-263.

<sup>10</sup> (a) S. K. Chattopadhyay, C. V. Kumar and P. K. Das, *J. Photochem.*, 1984, **24**, 1-9. (b) A. A. Gorman, I. Hamblett, C. Lambert, A. L. Prescott, M. A. J. Rodgers and H. M. Spence, *J. Am. Chem. Soc.*, 1987, **109**, 3091-3097.

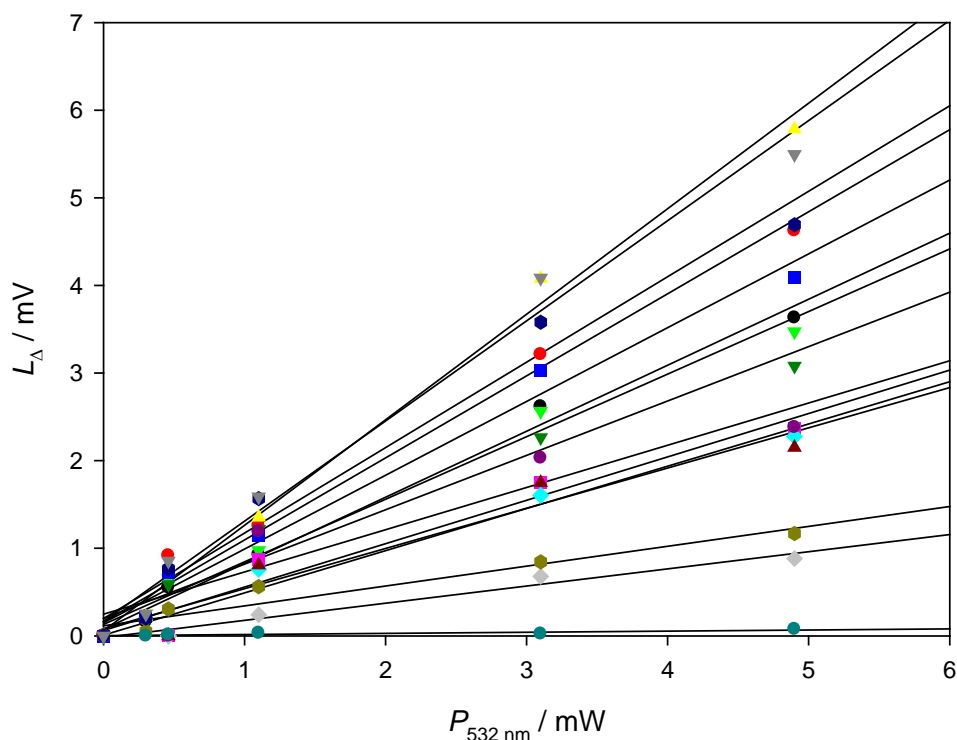


**Fig. 1.** Plot of singlet oxygen luminescence intensities extrapolated to zero time ( $L_{\Delta}$ ) as a function of the laser fluence at 532 nm ( $P_{532 \text{ nm}}$ ) for rose Bengal and the BODIPY sensitizers studied in this work in air-equilibrated acetonitrile. Compound: **RB** (●), **1** (●), **2** (▼), **3** (▲), **4** (■), **5** (■), **6** (◆), **7** (◆), **8** (▲), **9** (▼), **10** (◆), **11** (●), **12** (●), **13** (●), **14** (▼).

Dynamic quenching of photogenerated singlet oxygen by the BODIPY sensitizers was evaluated by measuring singlet oxygen emission lifetimes at 1270 nm in acetonitrile solutions. Stern-Volmer analysis allowed the determination of the bimolecular deactivation rate constants of singlet oxygen by the photosensitizing dye ( $k_{q\Delta}^{\text{Sens}}$ ) from eq. [3]:

$$\frac{\tau_{\Delta 0}}{\tau_{\Delta}} = 1 + k_{q\Delta}^{\text{Sens}} \times \tau_{\Delta 0} \times [\text{Sens}] \quad [3]$$

where  $\tau_{\Delta 0}$  is the emission lifetime of singlet oxygen photogenerated by the reference sensitizer phenalenone in acetonitrile (83.7  $\mu\text{s}$ ),<sup>11</sup>  $\tau_{\Delta}$  is the singlet oxygen emission lifetime measured in acetonitrile at least for five samples of each BODIPY sensitizer, and [Sens] is the concentration of BODIPY photosensitizer in  $\text{mol} \times \text{L}^{-1}$ . The Stern-Volmer constant is equal to  $k_{q\Delta}^{\text{Sens}} \times \tau_{\Delta 0}$ , and  $k_{q\Delta}^{\text{Sens}}$  can be determined from the slope of the corresponding Stern-Volmer plot ( $\tau_{\Delta 0}/\tau_{\Delta}$  vs. [Sens]).

Once  $k_{q\Delta}^{\text{Sens}}$  was known for each BODIPY sensitizer, absolute  $\Phi_{\Delta}$  values corrected for the  $^1\text{O}_2$  quenching by the sensitizer could be determined by using eq. [4] (where  $k_d = 1/\tau_{\Delta 0}$ ):<sup>12</sup>

$$\frac{\Phi_{\Delta}^{\text{app}}}{\Phi_{\Delta}} = \frac{k_d}{k_d + k_{q\Delta}^{\text{Sens}} \times [\text{Sens}]} \quad [4]$$

<sup>11</sup> O. Shimizu, J. Watanabe, K. Imakubo and S. Naito, *Chem. Lett.* 1999, 67-68.

<sup>12</sup> (a) D. Garcia-Fresnadillo, Y. Georgiadou, G. Orellana, A. M. Braun and E. Oliveros, *Helv. Chim. Acta*, 1996, **79**, 1996-1222. (b) I. Gutiérrez, S. G. Bertolotti, M. A. Biasutti, A. T. Soltermann and N. A. García, *Can. J. Chem.*, 1997, **75**, 423-428.

## 6. Calculation of the photodegradation rate constants and quantum yields.

The photodegradation quantum yields,  $\Phi_{pd}$ , were calculated according to the general equation [5]:

$$\Phi_{pd} = \frac{\text{number of degraded molecules}}{\text{number of photons absorbed}} \quad [5]$$

The photodegradation process of the compounds under study tends to show an asymptotic behavior with time, therefore, the analysis of the process has been carried out at short illumination times, when there is a linear relationship between the concentration of the compound and the irradiation time. The number of degraded molecules has been calculated from the decay in the BODIPYs concentration, taking into account the initial and the remaining absorbances in this linear region. Since the number of photons absorbed by the system changed during the irradiation time because in our experimental conditions there was no total absorption of the incident photons from the green LED lamp, and the optical density of the VIS absorption band of the BODIPYs decreased as the compound was photobleached, all these facts have been considered in order to calculate  $\Phi_{pd}$  accurately. From the linear regression analysis of the changes in compound concentration with irradiation time ( $[A]_t$ ), it is possible to calculate the remaining concentration (eq. [6], where  $[A]_0$  is the concentration of BODIPY at zero time and  $r$  the initial degradation rate) and, as a result, the absorbance minute by minute (considering the Lambert-Beer law, eq. [7]) could be calculated.

$$[A]_t = [A]_0 - r \cdot t \quad [6]$$

$$Abs_{\lambda,t} = \varepsilon_{\lambda} \cdot [A]_t \cdot l \quad [7]$$

The percentage of photons absorbed ( $F$ ) at each minute and for each illumination wavelength can be calculated by eq. [8].

$$F_{\lambda,t} = 1 - 10^{-Abs_{\lambda,t}} \quad [8]$$

As a consequence, the number of photons absorbed during a single minute ( $N_t$ ) can be calculated multiplying  $F$  by the photon flux at each wavelength,  $q_{p\lambda}$  (determined from the actinometry experiment using Reinecke's salt and the normalized emission spectrum of the green LED lamp) and  $N_t$  can be determined for the experimental interval of wavelengths by using eq. [9].

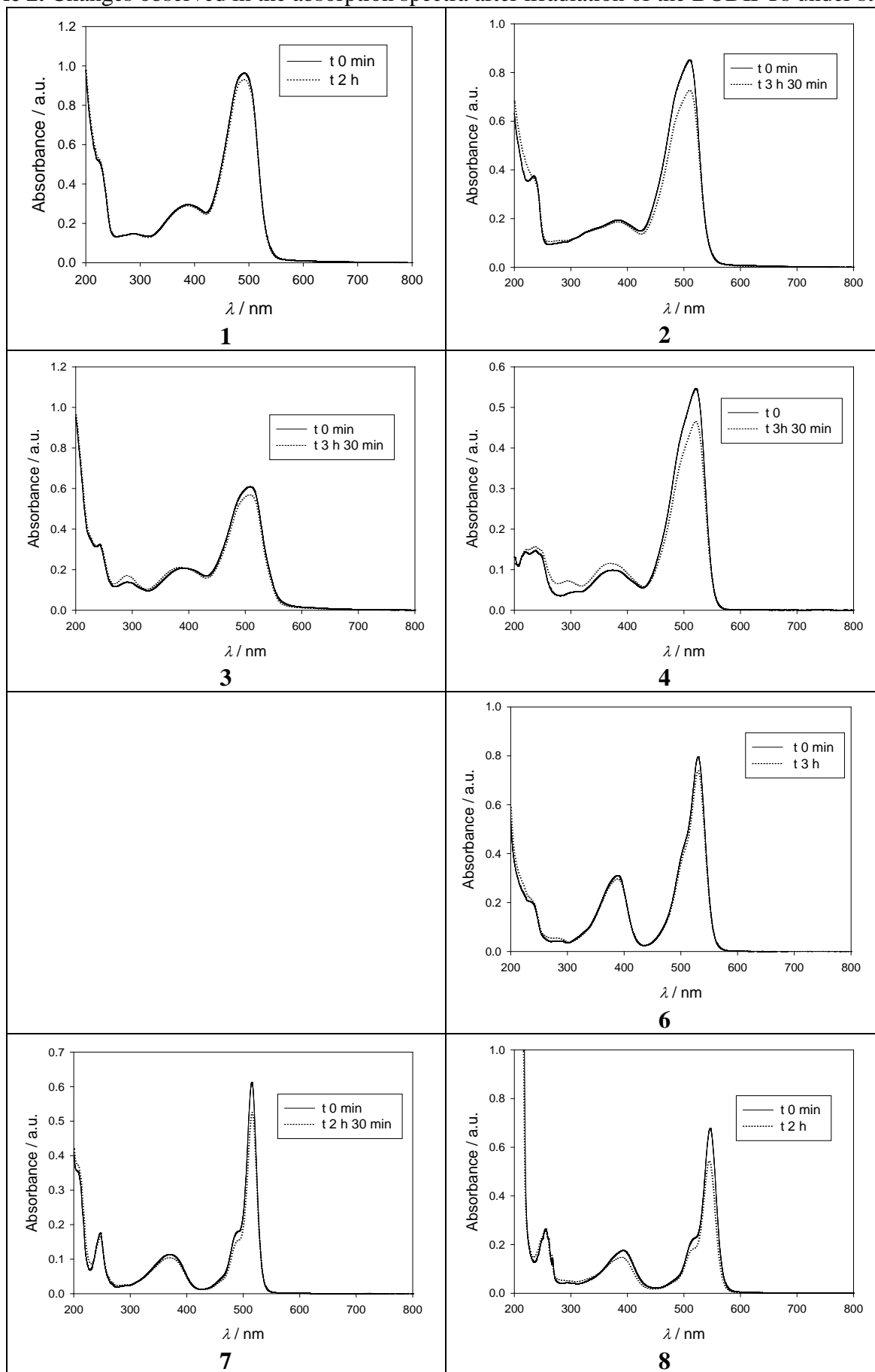
$$N_t = \sum_{\lambda=450\text{nm}}^{\lambda=600\text{nm}} F_{\lambda,t} \cdot q_{p\lambda} \quad [9]$$

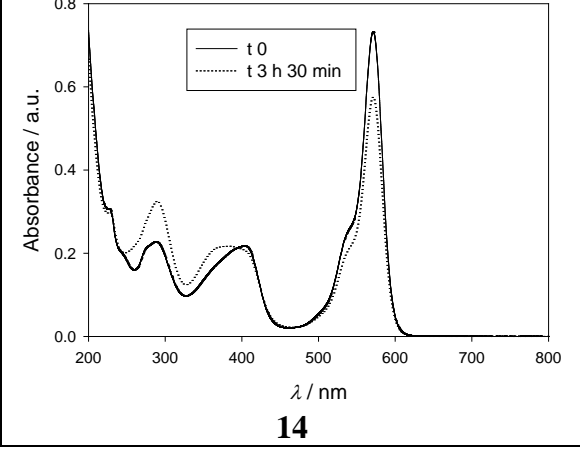
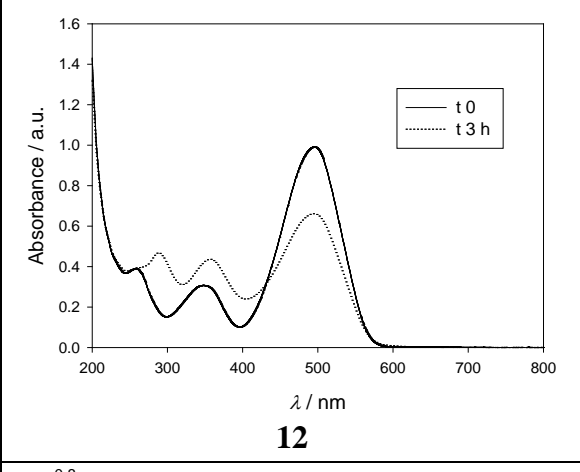
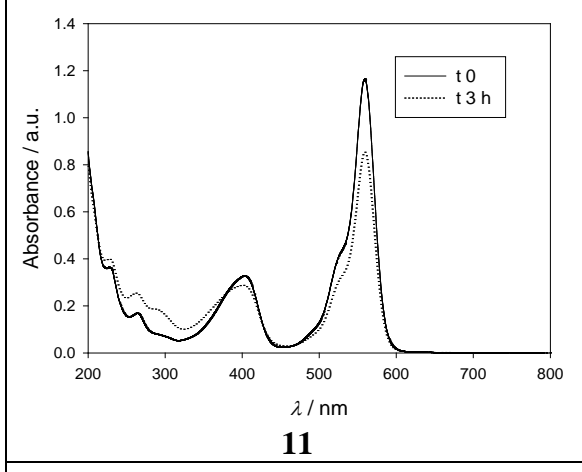
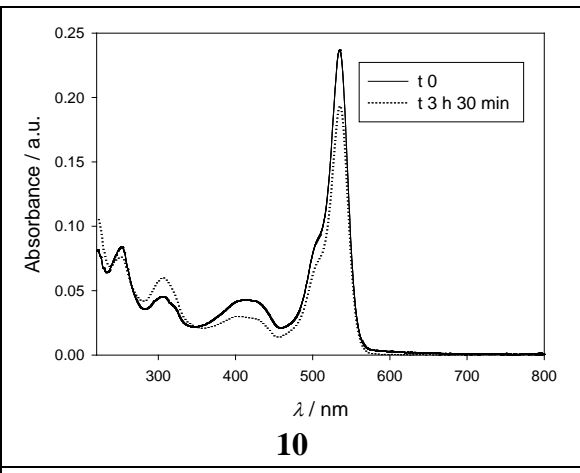
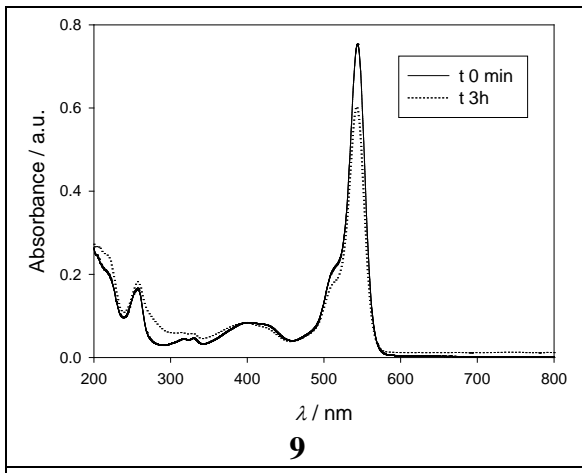
Following this procedure for the time interval considered (in minutes) during the photodegradation process, and adding the values obtained for each minute by applying eq. [10], it is possible to calculate the number of photons absorbed ( $N$ ) taking into account the observed absorbance decrease of the BODIPYs due to its photobleaching.

$$N = \sum_{t=0}^{t=final} N_t \quad [10]$$

Dye samples (3 mL, air equilibrated acetonitrile) were irradiated in a 1 cm light path quartz cell using a green LED lamp (GU10 green LED lamp, 230 V,  $\lambda_{em}^{max} = 515$  nm, FWHM = 33 nm).

**Table 2.** Changes observed in the absorption spectra after irradiation of the BODIPYs under study.





## 7. Chemical actinometry.

In order to determine the amount of photons from the green LED lamp ( $\lambda_{\text{em}}^{\text{max}} = 515 \text{ nm}$ , FWHM = 33 nm, Fig. 2) absorbed by the reaction geometry (quartz cells of 10 mm optical path length with a total volume of 3 mL), the following procedure was used:<sup>13</sup> Four samples were prepared, in complete absence of light, from a 0.15 M Reinecke's salt stock solution in distilled water. Each sample was added to a 10 mm quartz cell containing a 3 mm  $\times$  1 mm magnetic bar. The quartz cell was placed inside the box used for the irradiation experiments,<sup>8b</sup> and care was taken to assure reproducibility of the relative geometry with respect to the green LED lamp. The samples were exposed to green light for 60, 100, 120 and 160 s, respectively. A sample was kept in the dark as a control. After irradiation, aliquots of the irradiated sample and of the related control solution were diluted (4:1) into 0.1 M  $\text{Fe}(\text{NO}_3)_3$  in 0.5 M  $\text{HClO}_4$  solution, respectively. Thereafter, the absorbance of each solution at 450 nm was measured in quartz cells of 1 mm optical path length, in order to determine the amount of  $\text{SCN}^-$  produced as a result of the radiation absorbed by the illuminated system. A calibration graph was built by subtracting the absorbance of the controls to the corresponding irradiated sample (Fig. 3).

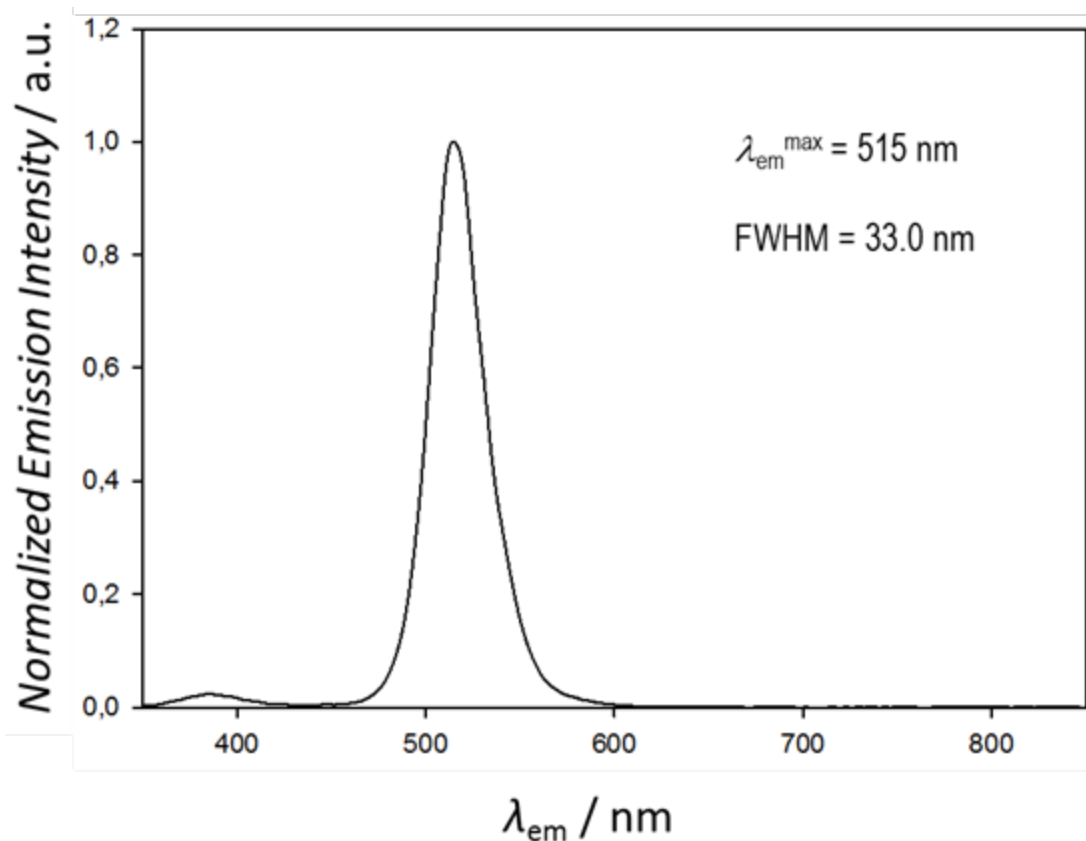


**Fig. 2.** Emission spectrum of the green LED lamp used in the photodegradation experiments.

<sup>13</sup> (a) H. J. Kuhn, S. E. Braslavsky and R. Schmidt, *Pure Appl. Chem.*, 2004, **76**, 2105-2146. (b) M. Montalti, A. Credi, L. Prodi and M. T. Gandolfi, *Handbook of Photochemistry*, 3rd ed.; CRC Press: Boca Raton, FL, 2006; Chapter 12, pp 601-616.

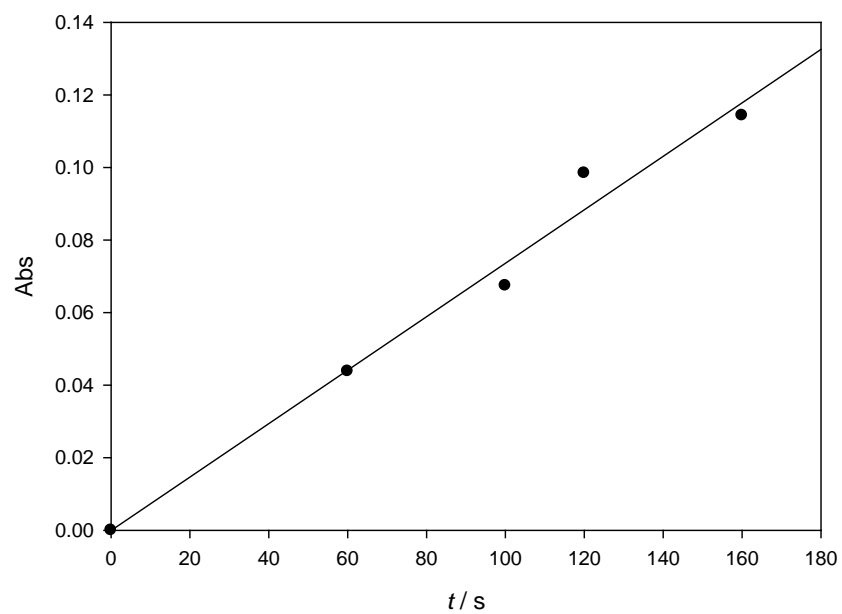


**Fig. 3.** Calibration graph of the chemical actinometry developed with the system used for the photodegradation experiments.

$$\text{Abs} = (7.4 \pm 0.6) \cdot 10^{-4} t - (0.04 \pm 0.06) \cdot 10^{-3}$$

$$r: 0.991$$

$$q_p = (2.2 \pm 0.2) \cdot 10^{-7} \text{ einstein} \cdot \text{s}^{-1}$$

## 8. Principal component analyses.

Principal Component Analysis (PCA) was carried out with Statgraphics Centurion XVII.

PCA is a statistical procedure that uses an orthogonal transformation to convert a set of observations of possibly correlated variables into a set of values of linearly uncorrelated variables called principal components (PCs). PCA is mainly used as a tool in exploratory data analysis and also for making predictive models. PCA is usually employed in order to reduce the amount of numerical data when there are correlations between them. For a sample characterized by  $n$  variables it is possible to build  $n$  principal components. Each PC is a linear combination of these variables, but the PCs are built in such a way that the first one accumulates the highest variance of the data, the second one has the next highest variance of the data, and so on. As a result, when there are correlations, the number of PCs is lower than the original variables and, generally, with two PCs, it is possible to analyse a relevant percentage of the variance. The resulting vectors are an uncorrelated orthogonal basis set and PCA is sensitive to the relative scaling of the original variables.

In this work, the studied variables have been: the presence of halogen atom in each position of the BODIPY core (Pos. X), the type of heavy atom (Br, I), the number of heavy atoms (nh), the singlet oxygen production quantum yield ( $\Phi_{\Delta}$ ), the quenching rate constant of  $^1\text{O}_2$  deactivation by the BODIPYs ( $k_{q\Delta}^{\text{Sens}}$ ), the photodegradation quantum yields ( $\Phi_{\text{pd}}$ ), and the initial photodegradation rates ( $r$ ). In order to specify the presence of a halogen group in a particular position, a binary system has been used (1 indicates the presence of halogen group and 0 the absence of halogen group). The same idea has been applied in order to discriminate between iodinated and brominated substituents (see the next table for compound **1** as an example).

Pos. 1	Pos. 2	Pos. 3	Pos. 5	Pos. 6	Pos. 7	Br	I	nh	$\Phi_{\Delta}$	$k_{q\Delta}^{\text{Sens}}$	$\Phi_{\text{pd}}$	$r$
1	1	0	0	0	0	1	0	2	0.90	0.30	5.8	1.6

In the PCA carried out in this work the variables have been standardized, i.e., they have the same variance and, as a result, the same importance in the analysis.